

Electrons and Phonons in amorphous Si: Deformation Potentials and Solutions of the Time Dependent Schrödinger Equation

D. A. Drabold and Jun Li

Department of Physics and Astronomy, Nanoscale and Quantum Phenomena Institute, Ohio University, Athens, OH 45701, U.S.A.

ABSTRACT

We employ first principles methods to explore the coupling between electrons and the lattice in amorphous silicon (a-Si). First we compute the adiabatic electronic response to phonon modes in a realistic model of a-Si. Then, we present a simulation of the electron dynamics of localized edge states in a-Si at room temperature by integrating the time dependent Schrödinger equation. We study the character of the spatial and spectral diffusion of the localized states and directly simulate and reveal the nature of thermally driven hopping. Phonon-induced resonant mixing leads to rapid electronic diffusion if states are available nearby in energy and real-space. We believe that many of the results we obtain are central to modeling transport involving localized states.

INTRODUCTION

It is of pure and applied interest to determine the nature of the coupling of the lattice and electron states in disordered materials. This interaction is the root of thermally driven hopping between localized states; this is the principal mechanism of conduction for virtually all disordered systems at sufficiently low temperatures. Anderson [1] first pointed out the failure of the conventional defect model in otherwise ordered structures to account for transport [2] phenomena in the disordered systems. Using a random lattice model, he gave a proof that without thermal activation the mobile entities will be localized and at low enough defect concentrations no diffusion takes place. Thomas [3] has argued that an electron starting in some localized state (as for example a donor) will suffer scattering with the phonons and become progressively delocalized. He showed with an Anderson model that this “phonon-induced delocalization” is essential to understanding transport in amorphous materials.

Previous thermal simulations with Born-Oppenheimer dynamics indicated that there is always a large electron-phonon coupling for the localized states in the band tails and in the optical gap [4]. The effects of thermal disorder on the quantum coherence of the localized states can only be computed by directly dealing with the electron dynamics from the time-dependent Schrödinger equation.

In this paper we use realistic Wooten-Weaire-Winer type models due to Djordjevic, Thorpe and Wooten (DTW) [5] which are in good agreement with the structural, electronic and vibrational properties of a-Si [6]. The electronic structure calculations are based upon “FIREBALL96” of Sankey and co-workers [7].

THEORY

A. Electron-Phonon Coupling

To infer the role of the electron-lattice coupling in a-Si we begin by computing a “deformation potential”, which measures the response of a certain electronic energy eigenvalue to a particular phonon. Earlier work has shown that it is useful to link the thermal fluctuation of the LDA energy eigenvalues near the band tails to the extent (localization) of the band tails in amorphous Si [4] (as separately measured in total yield photoemission experiments [8]). It is now routine in *ab initio* simulations to compute both the electronic and vibrational eigenvalues and eigenvectors. We show here that it is entirely straightforward to compute the electron-phonon coupling, a sort of “*ab initio* deformation potential”.

Consider a particular electronic eigenvalue, λ_n , say in one of the band tails in a-Si. To estimate the sensitivity of λ_n to a coordinate distortion (supposedly thermally induced), we can use the Hellmann-Feynman theorem, which gives $\partial\lambda_n/\partial\mathbf{R}_\alpha = \langle\psi_n|\partial\mathbf{H}/\partial\mathbf{R}_\alpha|\psi_n\rangle$. Then for small distortions $\delta\mathbf{R}_\alpha$, we have

$$\delta\lambda_n \approx \sum_\alpha \langle\psi_n|\partial\mathbf{H}/\partial\mathbf{R}_\alpha|\psi_n\rangle\delta\mathbf{R}_\alpha . \quad (1)$$

Here, \mathbf{R} is the 3N vector of displacements for all of the atomic coordinates from equilibrium and ψ_n is an eigenvector of \mathbf{H} . If the displacements $\delta\mathbf{R}_\alpha(t)$ arise from classical vibrations, then one can also write:

$$\delta\mathbf{R}_\alpha(t) = \sum_\omega A(T,\omega) \cos[\omega t + \phi_\omega]\chi_\alpha(\omega) , \quad (2)$$

where ω indexes the normal mode frequencies, $A(T,\omega)$ is the temperature dependent amplitude of the mode with frequency ω , ϕ_ω is an arbitrary phase, and $\chi_\alpha(\omega)$ is a normal mode with frequency ω and vibrational displacement index α . Using a temperature dependent squared amplitude $A^2(T,\omega)$, it is easy to see that the trajectory (long time) average of the expression for $\delta\lambda_n^2$ is:

$$\langle\delta\lambda_n^2\rangle \sim 1/2 \sum_\omega [A(T,\omega)\Xi_n(\omega)]^2 , \quad (3)$$

where the electron[n]-lattice[ω] coupling $\Xi_n(\omega)$ is given by:

$$\Xi_n(\omega) = \sum_\alpha \langle\psi_n|\partial\mathbf{H}/\partial\mathbf{R}_\alpha|\psi_n\rangle\chi_\alpha(\omega) . \quad (4)$$

Ξ is easily computed as a byproduct of any *ab initio* calculation of the vibrational modes [10].

For the case of DTW a-Si there are no coordination defects, though there are a small number of strained structures which lead to a reasonable distribution of localized tail and gap states. From figure 1 note that (1) the electron-phonon coupling is larger for conduction tail states than valence tail states (the conduction tails are also more localized), 2) the *acoustic* phonons are evidently more important to the tail states than optical phonons. 3) The electron-phonon coupling falls off rapidly for electron energies away from band edges.

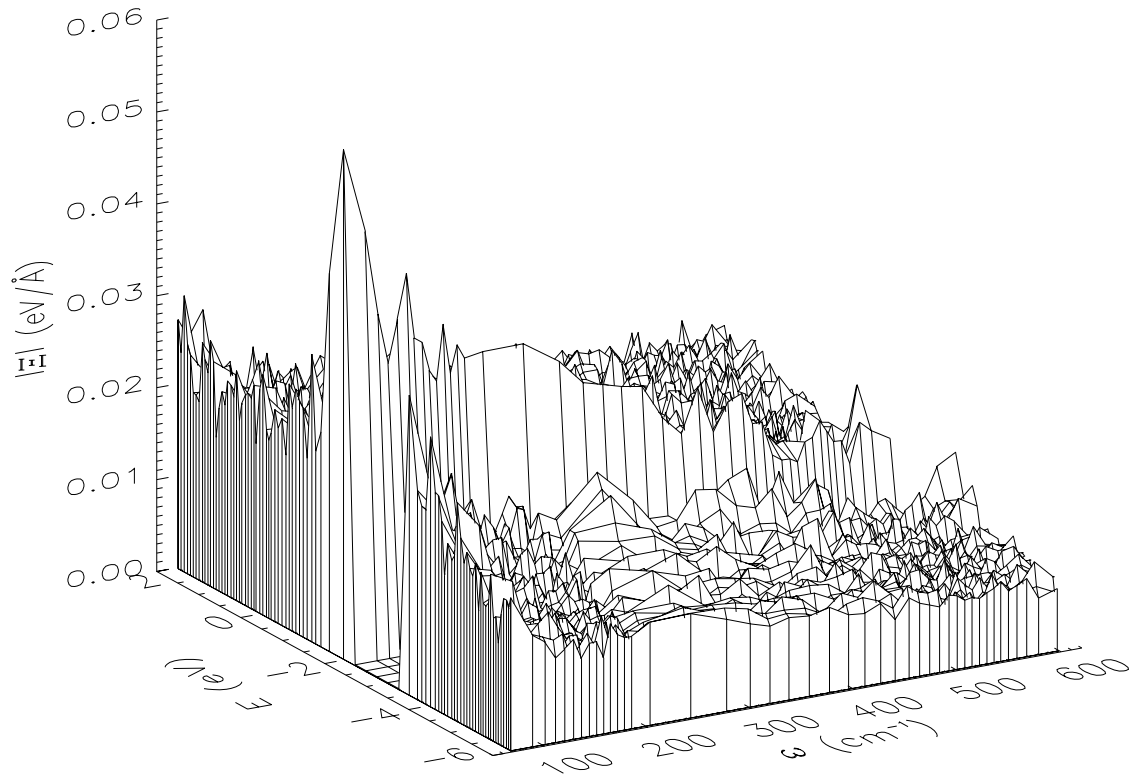


Figure 1. Electron-phonon coupling surface plot for 216 atom DTW model of amorphous Si. Phonon energy ω , electron energy E and absolute value of electron-phonon coupling Ξ (Equation 4). The optical gap extends from -3.45 to -2.11 eV. Note the dominance of *acoustic* phonons to the coupling.

Earlier work has emphasized a strong correlation between the localization of a gap or tail state (as measured by inverse participation ratio (IPR) [4]) and thermal fluctuation as gauged by RMS variation of eigenvalues. This appears to be a very general result and also occurs in chalcogenide glasses [9] and we suspect other materials with localized and bandtail states. In figure 2 we show histograms of the IPR and RMS thermal fluctuation for a simulation at 300K. This (possibly universal) correlation between a static property (localization) and dynamic property (thermal fluctuation) is helpful for interpreting experiments [8], and merits further analysis.

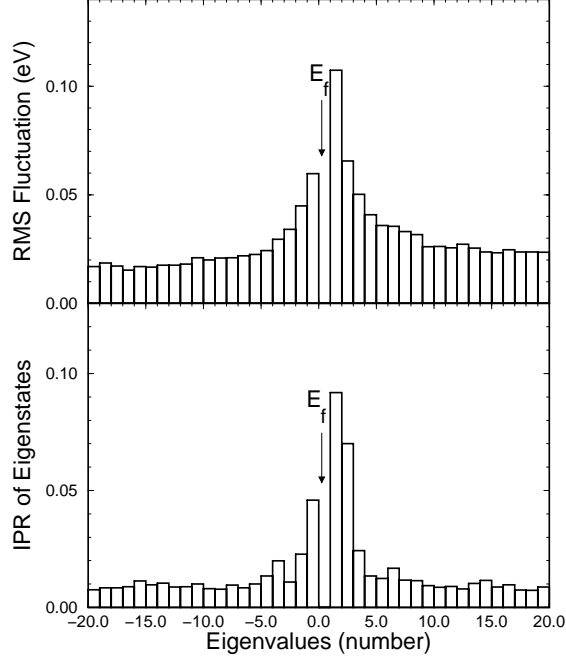


Figure 2. The localization (IPR) and the RMS fluctuation of gap vicinity energy eigenvalues at 300K (216 atom model, 1 ps time evolution). There is a strong correlation between the IPR (static property; bottom) and the thermal variation of the same eigenvalues (top panel). E_f is the Fermi level.

B. Time Dependent Schrödinger Equation

In this paper, we also explore a more fundamental direct integration of the time-dependent Schrödinger (Kohn-Sham) equation to characterize the dynamics of localized states in a small model of a-Si in the presence of thermal disorder (with $T=300\text{K}$). We employed Born-Oppenheimer dynamics for the ions and implemented the Crank-Nicholson [11] method along with the orthogonalization scheme of Tomfohr and Sankey [12] to obtain the time-dependence of a given state. The work discussed here is directly relevant to any system with disorder and therefore (potentially) localized states. One can understand this in fundamental terms as a step toward a 'realistic' solution of the finite-temperature Anderson problem [13].

We begin with the time-dependent Schrödinger equation:

$$i\hbar \frac{\partial}{\partial t} \Psi(t) = \hat{H}(t)\Psi(t) . \quad (5)$$

Here Ψ is the wavefunction of a single electron and \hat{H} is the one electron (density functional) Hamiltonian for the host (here, the model of a-Si). We explicitly compute the time-dependence of the Hamiltonian, which arises from ion motion obtained from the Born-Oppenheimer approximation. At each time step of the conventional quantum molecular dynamics (QMD) one can directly diagonalize the Hamiltonian matrix to obtain the stationary solution of the electronic structure. However the coherence of the electron state is lost in the solution. For any given initial state $\Psi(0)$, the wave function $\Psi(t)$ at time t can be obtained by solving the time-dependent Schrödinger equation or equivalently operating on the initial state with the time

evolution operator $\hat{U}(t)$, such that $\Psi(t) = \hat{U}(t)\Psi(0)$. In the Crank-Nicholson method, for sufficiently small step τ

$$\hat{U}(\tau) = (1 + i\tau \hat{H}/2\hbar)^{-1} (1 - i\tau \hat{H}/2\hbar). \quad (6)$$

For *any* τ , \hat{U} is exactly unitary, which also implies that all electron orbitals remain orthogonal for all later times. We calculated $\hat{U}(t)$ using $\hat{H}(t)$ with time dependence induced by thermal simulation for the ionic motion from Fireball96 [7]. With the Löwdin transformation [14] we express the wave function $\Psi(t)$ as a vector \mathbf{C} over an orthonormal basis ψ_i , $\Psi(t) = \sum C_i(t)\psi_i$. The key properties of localization and coherence do not change with the Löwdin transformation. We adopt the same approximation of Tomfohr and Sankey that for small enough time step τ , the Hamiltonian can be taken to be constant. Then the equivalent matrix equation becomes $i\hbar \partial/\partial t \mathbf{C}(t) = \mathbf{H}(t)\mathbf{C}(t)$. At room temperature, the results from the time step of 0.5 fs (for both ions and electrons) was found close to the results at a finer step 0.25fs at the test calculation. So the following results are based on the simulation at the time step 0.5 fs. These time steps appear to be very long; the reason these are acceptable is the proximity of the HOMO and LUMO eigenvalues to zero energy. If we began with a general wave packet built from the full spectral range of the basis, a much smaller τ would be required.

We performed the simulation on a 64-atom a-Si model. The localized states are associated with the geometrical defects and are located in the band gap. The highest occupied molecular orbital (HOMO) is spatially localized around a 3-fold dangling bond, essentially a *bandtail* state, only 0.1 eV higher than the next occupied orbital and near a dense collection of extended states. The lowest unoccupied molecular orbital (LUMO) is distributed around another small cluster associated with the floating bond. The LUMO of this model is spectrally a *midgap* state, isolated by 0.7 eV from both the lower HOMO and the next unoccupied state. Extended unoccupied states are at least 1.0 eV above the LUMO. We chose both HOMO and LUMO as the initial states to study their dynamics. Only the Γ point was used for Brillouin Zone sampling.

We have put a color figure on the WWW [15] which illustrates the spatial diffusion of the HOMO and LUMO states (a reduced monochrome figure acceptable for these Proceedings was found to be unsatisfactory). It is evident that the thermal disorder is sufficient to cause spatial diffusion of the original localized states, and the HOMO state diffuses far more rapidly than the LUMO. This result is very different (present work yielding more extended states) than the results for the ‘‘Born-Oppenheimer electron dynamics’’ [4], in which the simulation retained an unphysical coherence in the states, as the states are always computed anew at each step and are therefore always pure. Phonon-induced decoherence accumulates due to repeated phonon scattering events. Thus the time-dependent wave functions, $\mathbf{C}(t)$, will demonstrate quite different behavior from those wave functions obtained from conventional QMD. We employ the inverse participation ration (IPR) to measure the spatial distribution features, *i.e.*, localization, of a state: $\text{IPR} = \sum C_i^4$. Here C_i is the component of the state vector. For an extended state, IPR approaches $1/N$, where N is the number of basis. For an ideally localized state, IPR is unity instead.

Figure 3A provides the time development of the IPR of HOMO in the 5 ps simulation. The time-dependent solution of HOMO becomes extended very quickly. The trend is similar for the LUMO in figure 3B. The ‘‘turning-point’’ separating the stationary and dynamical IPR time development occurs near 350 fs for HOMO state. A similar departure develops only at 1.5 ps

for the LUMO state. The time-dependent solution of LUMO retains some of its initially localized character after 5 ps of simulation because it is more separated at 300K than the HOMO from a reservoir of like energy states with which to mix.

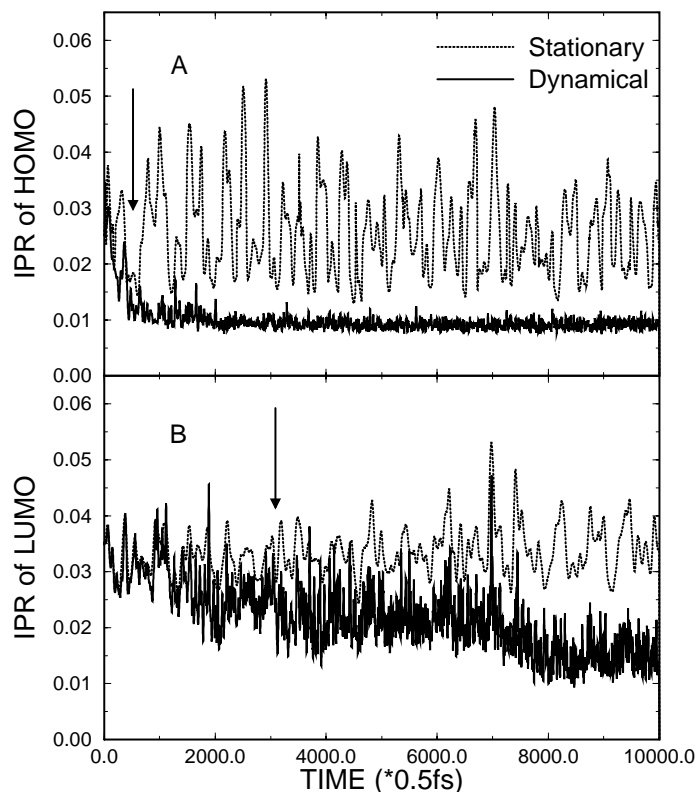


Figure 3. The evolution of the localization (IPR) of the original A.) HOMO and B.) LUMO. The dotted line is for the stationary solution (Born-Oppenheimer) and the solid line for the dynamical (time-dependent Schrödinger equation) solution. Arrows indicate the departure of the adiabatic and time dependent Schrödinger solutions. $T = 300\text{K}$.

Electronic diffusion is understood qualitatively as a consequence of quantum mechanical mixing when another state gets close in energy (and real space) to a reference eigenstate whose evolution we are tracking [16]. The mixing naturally leads to less localized states and this continues in principle until the packet has diffused throughout the simulation cell. We now go further to investigate the spectral diffusion of the electron state into nearby (almost resonant) states. Since the structure fluctuates at moderate fixed temperature, the Hamiltonian can be viewed as perturbed around an average H_0 . With reference to the initial eigenspace of the Hamiltonian the transition amplitude to state α is proportional to the probability of finding an eigenvector in the initial eigenspace, *i.e.*, $\rho(\alpha) \propto |\langle C_\alpha(0) | C(t) \rangle|^2$, where α is the eigenstate label in the initial eigenspace. Here we are interested in the transition to the states around the gap region, which are the most important states for transport near the so-called mobility edges, which marks the transition from localized to delocalized states at zero temperature. The mobility edge is destroyed by the thermal fluctuations.

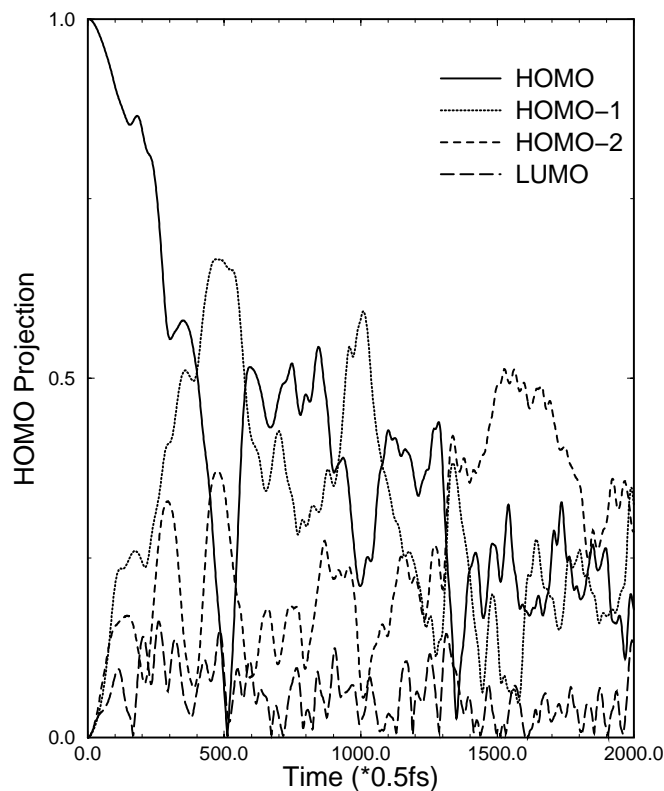


Figure 4. The spectral evolution of the dynamical HOMO state, and its “phonon-induced leakage” into neighboring energy states similar to figure 5 where the initial state is LUMO. $T = 300\text{K}$.

Figure 4 depicts the first 1 ps evolution of the transition or hopping probabilities from the HOMO to nearby states. The component of the original ($t=0$) HOMO decreases to zero within 250 fs (earlier than the 350 fs IPR turning-point), which indicates that the decoherence is very fast for the HOMO. The valence state just below the HOMO reaches its maximum as the HOMO approaches its first minimum at about 250 fs. The second valence state below the HOMO reaches its maximum at about 750 fs, 0.5 ps later than the first valence state below the HOMO. Spectrally, the original HOMO diffuses into other valence states at a rate related to the thermal activation. A small portion of transfer occurs even between the HOMO and LUMO. The magnitude of the transition across the gap is far lower than the transition from the HOMO to other valence bands. *This is a quantum effect associated with the huge electron-phonon coupling of the localized states, since the room temperature (~ 26 meV) cannot directly induce a transition between the HOMO and LUMO with a gap of 0.6 eV.* The tunneling or spatial overlap between the hopping states may play another important role in the deeper gap transition besides the thermal activation. The diffusion of the LUMO to its nearest unoccupied localized state (0.7 eV above) gives a direct indication of the hopping diffusion in figure 5. The character of LUMO is different from the HOMO. The spectral diffusion from LUMO is slower than that of HOMO as shown in figure 5. It is similar to the extent that the LUMO diffuses into the neighboring conduction states more readily than across the gap and the spectral diffusion is also strongly dependent on the distance between the LUMO and other conduction states.

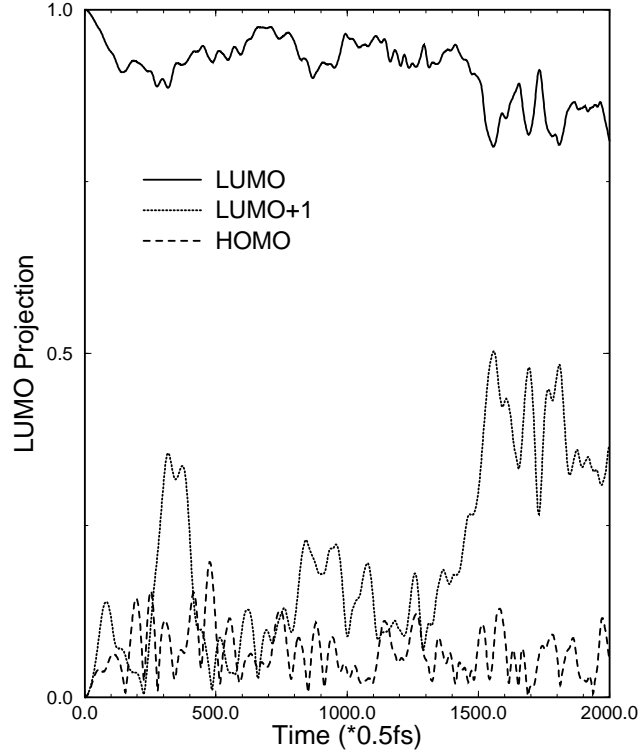


Figure 5. The spectral evolution of the dynamical LUMO state. $T=300\text{K}$.

We found that these two different localized states demonstrate different response to thermal manipulation and this difference is very different from the results of Born-Oppenheimer dynamics. The HOMO is easily delocalized by the thermal disturbance while the delocalizing progress is very slow for LUMO. Previous Born-Oppenheimer dynamics [4] showed that the eigenvalue of LUMO has larger fluctuation than the HOMO. However, the time coherence in the dynamical solution reveals the different delocalization process because of the difference in spectral and spatial “neighborhoods” of the states studied. We have noted that the delocalization will not occur if the temperature is too close to 0 K.

CONCLUSION

In this paper, we presented a simulation of the dynamics of the localized electronic edge states in a-Si at room temperature by integrating the time dependent Schrödinger equation with a simple Crank-Nicholson method and a first-principles (Fireball96) Hamiltonian. We found that the localized edge states, the highest occupied orbital (HOMO) and the lowest unoccupied orbital (LUMO), are strongly modulated by phonons. Temperature induces a stronger intra-band transition than the inter-band transition across the gap. The simulation indicates a different diffusion mechanism in HOMO and LUMO. We emphasize that the decoherence is a dynamical process and can only be approached by the analysis of electron dynamics. The observed delocalization is also a dynamical effect, which will not occur if the adiabatic approach is adopted, since the memory of the phase of a quantum state is discarded.

This paper is far from the final word: one key point will be to ascertain the extent to which we are sampling the bandtail states in “real” a-Si. Our small model quite probably is inadequate here, and larger calculations are underway. We believe however that the basic physical processes are present in this paper. Our work demonstrates in a quantitative and realistic way (1) the nature of thermally induced hopping, (2) the need for spatial and spectral overlap for electronic diffusion and (3) lays important groundwork for a future theory of non-adiabatic transport in disordered systems.

ACKNOWLEDGMENTS

This work was supported in part by the National Science Foundation under grants DMR 00-81006 and DMR-00-74624. We thank Prof. N. Mousseau for providing the 64 atom a-Si model for this work and we thank Prof. O. F. Sankey and Dr. Serge Nakhmanson for helpful discussions. We further thank Mrs. Pranoat Suntharothok-Priesmeyer for help with the manuscript. This work owes much to Dr. Peter Thomas, whose work motivated these calculations.

REFERENCES

1. P. W. Anderson, Phys. Rev. **109**, 1492 (1958).
2. For an example of recent work on quantum transport see, A. Demkov, X. Zhang and D. A. Drabold, Phys. Rev. B **64**, 125306 (2001), and references therein.
3. P. Thomas, “Electronic transport in disordered Semiconductors” in *Insulating and semiconducting glasses*, ed. P. Boolchand, (World Scientific, Singapore 2000), p. 553.
4. D. A. Drabold, P. A. Fedders, Stefan Klemm and O. F. Sankey, Phys. Rev. Lett. **67**, 2179 (1991); D. A. Drabold and P. A. Fedders, Phys. Rev. B **60**, R721, (1999); D. A. Drabold, J. Non.-Cryst. Sol. **266**, 211 (2000).
5. B. R. Djordjevic *et al.*, Phys. Rev. B, **52**, 5685 (1995); F. Wooten and D. Weaire, *Solid State Physics*, edited by H. Ehrenreich and D. Turnbull (Academic Press, New York, 1991), Vol. 40, p.2
6. P. A. Fedders, D. A. Drabold and S. N. Nakhmanson, Phys. Rev. B **58**, 15624 (1998).
7. A. Demkov, J. Ortega, O. F. Sankey, and M. Grumbach, Phys. Rev. B **52**, 1618 (1995).
8. S. Aljishi, J. D. Cohen, S. Jin, and L. Ley, Phys. Rev. Lett. **64**, 2811 (1990).
9. M. Cobb and D. A. Drabold, Phys. Rev. B **56**, 3054 (1997).
10. D. A. Drabold in *Properties and Applications of Amorphous Materials*, ed. by M. F. Thorpe and L. Tichy, (Kluwer, Dordrecht, 2001).
11. L. Garcia, *Numerical Methods for Physics*, (Prentice Hall, 1994) Chap.8, pp. 244-246.
12. J. K. Tomfohr and O. F. Sankey, Phys. Stat. Sol. **226**, 115 (2001).
13. N. F. Mott and E. A. Davis, *Electronic Processes in Non-Crystalline Materials*, 2nd. edition (Clarendon, Oxford, 1979).
14. P. O. Löwdin, Adv. Quantum Chem. **5**, 185 (1970).
15. <http://www.phy.ohiou.edu/~drabold>; See also J. Li and D. A. Drabold, Phys. Stat. Sol. (in press).
16. Jianjun Dong and D. A. Drabold, Phys. Rev. Lett. **80**, 1928 (1998).